

MODIFIED NODAL INTEGRAL METHOD FOR THE THREE-DIMENSIONAL, TIME-DEPENDENT, INCOMPRESSIBLE NAVIER-STOKES EQUATIONS

Fei Wang and Rizwan-uddin

Department of Nuclear, Plasma and Radiological Engineering
University of Illinois at Urbana-Champaign
Urbana, IL 61801 USA

feiwang1@uiuc.edu, rizwan@uiuc.edu

ABSTRACT

Modified nodal integral method (MNIM) for two-dimensional, time-dependent Navier-Stokes (N-S) equations is extended to three dimensions. Nodal integral method (NIM) is based on local transverse-integrations over finite size cells that reduce each partial differential equation (PDE) to a set of ordinary differential equations (ODEs). Solutions of these ODEs in each cell for the transverse-averaged dependent variables are then utilized to develop the difference schemes. The discrete variables are scalar velocities and pressure, averaged over the faces of brick-like cells. The development of MNIM is different from conventional nodal method in two ways: i) it is Poisson-type pressure equation based; ii) the convection terms are retained on the left hand side of the transverse-integrated equations, and thus contribute to the homogeneous part of the solution. The first feature leads to a set of symmetric transverse-integrated equations for all the velocities, and the second feature yields distributions of *constant + linear + exponential* form for the transverse-averaged velocities. The scheme is tested on three-dimensional lid-driven cavity problem in cubic and prism shaped cavities. Results obtained using MNIM on fairly coarse meshes are comparable with reference solutions obtained using much finer meshes.

Key Words: Navier-Stokes, difference equations, nodal method, coarse-mesh, inherent upwinding

1. INTRODUCTION

Nodal methods have been developed over the last two decades to solve the Navier-Stokes equations [1-5]. Recent developments of nodal integral methods for fluid flow problems show improvements in efficiency over more conventional approaches similar to those shown by nodal methods developed for the neutronics problems. (A review of nodal methods developed in the nuclear industry is given by Lawrence [6].) Applying coarse mesh methods to N-S equations promises solution of much larger scale fluid dynamics problems as well as direct numerical simulation (DNS) of turbulent flow. Two-dimensional modified nodal integral method has been developed recently [5] with two new features: Poisson-type pressure equation was used instead of the continuity equation; convection terms in the N-S equations are kept on the left hand side and thus contribute to the homogeneous solution of the transverse-integrated ordinary differential equations. Here, we extend the two-dimensional modified nodal integral method to three dimensions. The extension is straightforward but not trivial.

Usually, NIM is limited to domain with boundaries parallel to one of the Cartesian axis. However, to overcome the geometry limitation, nodal integral methods have been extended to arbitrary geometries recently [7]. A similar approach can be used to develop MNIM for the three-dimensional N-S equations for arbitrary geometries.

A note on terminology: Since the term “node” is in high demand (in the NIM, it is used to represent a finite volume in the space of independent variables; it represents a point in space in finite difference and finite volume methods; and it is also used to represent a processor or a group of processors for parallel computation of CFD problems), in this paper we will use the term “cell” to denote what was called a “node” by Azmy and Dorning [1] when they developed their nodal integral method for the Navier-Stokes equations.

2. DEVELOPMENT OF THE MODIFIED NODAL INTEGRAL METHOD

2.1. Reformulation of the N-S Equations

The time-dependent, incompressible Navier-Stokes equations are:

$$\frac{\partial u}{\partial X} + \frac{\partial v}{\partial Y} + \frac{\partial w}{\partial Z} = 0 \quad (1)$$

$$\frac{\partial u}{\partial T} + u \frac{\partial u}{\partial X} + v \frac{\partial u}{\partial Y} + w \frac{\partial u}{\partial Z} - \nu \left[\frac{\partial^2 u}{\partial X^2} + \frac{\partial^2 u}{\partial Y^2} + \frac{\partial^2 u}{\partial Z^2} \right] + \frac{1}{\rho} \frac{\partial p}{\partial X} - g_x(X, Y, Z, T) = 0 \quad (2)$$

$$\frac{\partial v}{\partial T} + u \frac{\partial v}{\partial X} + v \frac{\partial v}{\partial Y} + w \frac{\partial v}{\partial Z} - \nu \left[\frac{\partial^2 v}{\partial X^2} + \frac{\partial^2 v}{\partial Y^2} + \frac{\partial^2 v}{\partial Z^2} \right] + \frac{1}{\rho} \frac{\partial p}{\partial Y} - g_y(X, Y, Z, T) = 0 \quad (3)$$

$$\frac{\partial w}{\partial T} + u \frac{\partial w}{\partial X} + v \frac{\partial w}{\partial Y} + w \frac{\partial w}{\partial Z} - \nu \left[\frac{\partial^2 w}{\partial X^2} + \frac{\partial^2 w}{\partial Y^2} + \frac{\partial^2 w}{\partial Z^2} \right] + \frac{1}{\rho} \frac{\partial p}{\partial Z} - g_z(X, Y, Z, T) = 0 \quad (4)$$

where, $g(X, Y, Z, T)$ represents volumetric sources such as gravity, and capital letters X, Y, Z and T are used to denote the global coordinates. To develop a numerical scheme, very often a Poisson equation for pressure is used instead of the continuity equation. Manipulating Equations (2-4), the Poisson equation for pressure is given by

$$\begin{aligned} \frac{\partial^2 p}{\partial X^2} + \frac{\partial^2 p}{\partial Y^2} + \frac{\partial^2 p}{\partial Z^2} = & -\rho \left[\left(\frac{\partial u}{\partial X} \right)^2 + \left(\frac{\partial v}{\partial Y} \right)^2 + \left(\frac{\partial w}{\partial Z} \right)^2 \right] \\ & - 2\rho \frac{\partial u}{\partial Y} \frac{\partial v}{\partial X} - 2\rho \frac{\partial v}{\partial Z} \frac{\partial w}{\partial Y} - 2\rho \frac{\partial w}{\partial X} \frac{\partial u}{\partial Y} + \rho \frac{\partial g_x}{\partial X} + \rho \frac{\partial g_y}{\partial Y} + \rho \frac{\partial g_z}{\partial Z} \\ & - \rho \left[\frac{\partial D}{\partial T} + u \frac{\partial D}{\partial X} + v \frac{\partial D}{\partial Y} + w \frac{\partial D}{\partial Z} - \nu \frac{\partial^2 D}{\partial X^2} - \nu \frac{\partial^2 D}{\partial Y^2} - \nu \frac{\partial^2 D}{\partial Z^2} \right] \end{aligned} \quad (5)$$

where, the dilatation term D is given by

$$D \equiv \frac{\partial u}{\partial X} + \frac{\partial v}{\partial Y} + \frac{\partial w}{\partial Z} . \quad (6)$$

Since equation (5) was derived only from the momentum equations (2-4), the continuity equation can be incorporated in equation (5) by simply setting D equal to zero. But, as reported [8,9], this may cause numerical instability in the scheme. In the modified nodal integral method, keeping only the temporal derivative term, $\frac{\partial D}{\partial T}$, while setting the other terms in the bracket to zero leads to a stable scheme.

In the nodal method, the space-time domain (X, Y, Z, T) is first discretized into rectangular space-time cells (i, j, k, n) of size $(2a_i \times 2b_j \times 2c_k \times 2\tau_n)$ with cell-centered *local coordinates* $(-a_i \leq x \leq a_i, -b_j \leq y \leq b_j, -c_k \leq z \leq c_k, -\tau_n \leq t \leq \tau_n)$. The N-S equations are re-written in terms of local coordinates:

$$\begin{aligned} & \frac{\partial u}{\partial t} + u_p \frac{\partial u}{\partial x} + v_p \frac{\partial u}{\partial y} + w_p \frac{\partial u}{\partial z} - v \left[\frac{\partial^2 u}{\partial x^2} + \frac{\partial^2 u}{\partial y^2} + \frac{\partial^2 u}{\partial z^2} \right] \\ &= -\frac{1}{\rho} \frac{\partial p}{\partial x} + g_x(x, y, z, t) - (u - u_p) \frac{\partial u}{\partial x} - (v - v_p) \frac{\partial u}{\partial y} - (w - w_p) \frac{\partial u}{\partial z} \end{aligned} \quad (7)$$

$$\begin{aligned} & \frac{\partial v}{\partial t} + u_p \frac{\partial v}{\partial x} + v_p \frac{\partial v}{\partial y} + w_p \frac{\partial v}{\partial z} - v \left[\frac{\partial^2 v}{\partial x^2} + \frac{\partial^2 v}{\partial y^2} + \frac{\partial^2 v}{\partial z^2} \right] \\ &= -\frac{1}{\rho} \frac{\partial p}{\partial y} + g_y(x, y, z, t) - (u - u_p) \frac{\partial v}{\partial x} - (v - v_p) \frac{\partial v}{\partial y} - (w - w_p) \frac{\partial v}{\partial z} \end{aligned} \quad (8)$$

$$\begin{aligned} & \frac{\partial w}{\partial t} + u_p \frac{\partial w}{\partial x} + v_p \frac{\partial w}{\partial y} + w_p \frac{\partial w}{\partial z} - v \left[\frac{\partial^2 w}{\partial x^2} + \frac{\partial^2 w}{\partial y^2} + \frac{\partial^2 w}{\partial z^2} \right] \\ &= -\frac{1}{\rho} \frac{\partial p}{\partial z} + g_z(x, y, z, t) - (u - u_p) \frac{\partial w}{\partial x} - (v - v_p) \frac{\partial w}{\partial y} - (w - w_p) \frac{\partial w}{\partial z} \end{aligned} \quad (9)$$

$$\begin{aligned} & \frac{\partial^2 p}{\partial x^2} + \frac{\partial^2 p}{\partial y^2} + \frac{\partial^2 p}{\partial z^2} = -\rho \left[\left(\frac{\partial u}{\partial x} \right)^2 + \left(\frac{\partial v}{\partial y} \right)^2 + \left(\frac{\partial w}{\partial z} \right)^2 \right] \\ & - 2\rho \frac{\partial u}{\partial y} \frac{\partial v}{\partial x} - 2\rho \frac{\partial v}{\partial z} \frac{\partial w}{\partial y} - 2\rho \frac{\partial w}{\partial x} \frac{\partial u}{\partial y} + \rho \frac{\partial g_x}{\partial x} + \rho \frac{\partial g_y}{\partial y} + \rho \frac{\partial g_z}{\partial z} - \rho \frac{\partial D}{\partial t} \end{aligned} \quad (10)$$

where u_p , v_p and w_p are respectively the cell-averaged u , v and w velocities at the previous time step. Equations (7-9) are different from the standard momentum equations (equations (2-4)) in that convection terms based on cell-averaged velocities at the previous time step have been added on both sides of the equations and the original convection terms are moved to the right hand side. The reason behind writing the momentum equations in this form is to reduce the computational burden that results if the nonlinearity of the convection term (at the current time step) is resolved iteratively.

2.2. Transverse Integration Procedure

Time, in this modified nodal scheme, is treated in the same fashion as spatial coordinates.

By applying the *local* transverse integration procedure, such as

$$\bar{\phi}_{i,j,k,n}^{xyt}(z) \equiv \frac{1}{8a_i b_j \tau_n} \int_{-\tau_n}^{\tau_n} \int_{-b_j}^{b_j} \int_{-a_i}^{a_i} \phi_{i,j,k}(x, y, z, t) dx dy dt, \quad \phi = u, v, w, p \quad (11)$$

to equations (7-10), fifteen transverse-integrated ordinary differential equations are obtained,

$$\frac{d^2 \bar{p}^{yzt}(x)}{dx^2} = \bar{S}_1^{yzt}(x) \quad (12)$$

$$\frac{d^2 \bar{p}^{xzt}(y)}{dy^2} = \bar{S}_1^{xzt}(y) \quad (13)$$

$$\frac{d^2 \bar{p}^{xyt}(z)}{dz^2} = \bar{S}_1^{xyt}(z) \quad (14)$$

$$u_p \frac{d\bar{u}^{yzt}(x)}{dx} - v \frac{d^2 \bar{u}^{yzt}(x)}{dx^2} = \bar{S}_2^{yzt}(x) \quad (15)$$

$$u_p \frac{d\bar{v}^{yzt}(x)}{dx} - v \frac{d^2 \bar{v}^{yzt}(x)}{dx^2} = \bar{S}_3^{yzt}(x) \quad (16)$$

$$u_p \frac{d\bar{w}^{yzt}(x)}{dx} - v \frac{d^2 \bar{w}^{yzt}(x)}{dx^2} = \bar{S}_4^{yzt}(x) \quad (17)$$

$$v_p \frac{d\bar{u}^{xzt}(y)}{dy} - v \frac{d^2 \bar{u}^{xzt}(y)}{dy^2} = \bar{S}_2^{xzt}(y) \quad (18)$$

$$v_p \frac{d\bar{v}^{xzt}(y)}{dy} - v \frac{d^2 \bar{v}^{xzt}(y)}{dy^2} = \bar{S}_3^{xzt}(y) \quad (19)$$

$$v_p \frac{d\bar{w}^{xzt}(y)}{dy} - v \frac{d^2 \bar{w}^{xzt}(y)}{dy^2} = \bar{S}_4^{xzt}(y) \quad (20)$$

$$w_p \frac{d\bar{u}^{xyt}(z)}{dz} - v \frac{d^2 \bar{u}^{xyt}(z)}{dz^2} = \bar{S}_2^{xyt}(z) \quad (21)$$

$$w_p \frac{d\bar{v}^{xyt}(z)}{dz} - v \frac{d^2 \bar{v}^{xyt}(z)}{dz^2} = \bar{S}_3^{xyt}(z) \quad (22)$$

$$w_p \frac{d\bar{w}^{xyt}(z)}{dz} - v \frac{d^2 \bar{w}^{xyt}(z)}{dz^2} = \bar{S}_4^{xyt}(z) \quad (23)$$

$$\frac{d\bar{u}^{xyz}(t)}{dt} = \bar{S}_2^{xyz}(t) \quad (24)$$

$$\frac{d\bar{v}^{xyz}(t)}{dt} = \bar{S}_3^{xyz}(t) \quad (25)$$

$$\frac{d\bar{w}^{xyz}(t)}{dt} = \bar{S}_4^{xyz}(t) \quad (26)$$

where the subscripts (i, j, k, n) on independent variables have been omitted, and terms not explicit are lumped into the right hand as pseudo-source terms. For example,

$$\bar{S}_1^{zxt}(y) \equiv -\frac{1}{8c_k a_i \tau_n} \int_{-\tau_n}^{\tau_n} \int_{-a_i}^{a_i} \int_{-c_k}^{c_k} dz dx dt \left(\begin{array}{l} -\frac{\partial^2 p}{\partial x^2} - \frac{\partial^2 p}{\partial z^2} - \rho \left[\left(\frac{\partial u}{\partial x} \right)^2 + \left(\frac{\partial v}{\partial y} \right)^2 + \left(\frac{\partial w}{\partial z} \right)^2 \right] \\ -2\rho \frac{\partial u}{\partial y} \frac{\partial v}{\partial x} - 2\rho \frac{\partial v}{\partial z} \frac{\partial w}{\partial y} - 2\rho \frac{\partial w}{\partial x} \frac{\partial u}{\partial y} \\ +\rho \frac{\partial g_x}{\partial x} + \rho \frac{\partial g_y}{\partial y} + \rho \frac{\partial g_z}{\partial z} - \rho \frac{\partial D}{\partial t} \end{array} \right) \quad (27)$$

Notice that the transverse-integrated equations (12-26) are similar in form as those obtained in the two-dimensional MNIM [5].

2.3. Local Solutions for the Transverse-Integrated ODEs

The ODEs are solved analytically within each cell. Particular solutions are obtained after expanding and truncating the modified pseudo-source terms at the zeroth order. [In general, truncating at higher order, in conjunction with other consistent approximations, leads to numerical scheme of order higher than second.] The local solutions of the ODEs for transverse-integrated pressure are quadratic, and for example, the solution for $\bar{p}^{zxt}(y)$ is given by

$$\bar{p}^{zxt}(y) = \frac{\bar{S}_1^{zxt}}{2} y^2 + C_1 y + C_2 \quad (28)$$

The local solutions for $\bar{u}^{zxt}(y)$ are of the following form.

$$\bar{u}^{zxt}(y) = \bar{S}_2^{zxt} e^{\frac{v_p y}{v}} + C_3 y + C_4 \quad (29)$$

Solutions for the other transverse-integrated velocities ($\bar{u}^{yzt}(x)$, $\bar{u}^{xyt}(z)$, $\bar{v}^{yzt}(x)$, $\bar{v}^{zxt}(y)$, $\bar{v}^{xyt}(z)$, $\bar{w}^{yzt}(x)$, $\bar{w}^{zxt}(y)$, $\bar{w}^{xyt}(z)$) are of similar forms. The solutions for $\bar{u}^{xyz}(t)$, $\bar{v}^{xyz}(t)$ and $\bar{w}^{xyz}(t)$ are linear in time. The constants C_i ($i = 1, 2, \dots$) are eliminated in favor of the discrete unknowns by imposing boundary conditions on cell surfaces normal to the independent variables. A set of discrete equations is obtained by imposing continuity of each variable (and its derivative for the second order ODEs) at cell interfaces. This process leads to a set of fifteen coupled, algebraic equations per cell for \bar{u}_{ijk}^{yzt} , \bar{v}_{ijk}^{yzt} , \bar{w}_{ijk}^{yzt} , \bar{p}_{ijk}^{yzt} , \bar{u}_{ijk}^{zxt} , \bar{v}_{ijk}^{zxt} , \bar{w}_{ijk}^{zxt} , \bar{p}_{ijk}^{zxt} , \bar{u}_{ijk}^{xyt} , \bar{v}_{ijk}^{xyt} , \bar{w}_{ijk}^{xyt} , \bar{p}_{ijk}^{xyt} , \bar{u}_{ijk}^{xyz} , \bar{v}_{ijk}^{xyz} , \bar{w}_{ijk}^{xyz} , in terms of the fifteen pseudo-source terms, S 's.

2.4. Constraint Equations

Following the procedures for NIM, the pseudo-source terms are eliminated next using fifteen constraint equations. Four constraint equations are obtained by applying the operator,

$\frac{1}{16a_i b_j c_k \tau_n} \int_{-\tau_n}^{\tau_n} \int_{-c_k}^{c_k} \int_{-b_j}^{b_j} \int_{-a_i}^{a_i} dx dy dz dt$, on Eqs. (7-10). The other eleven constraint equations are

obtained by imposing the condition that the cell-averaged variables be unique, independent of the order of integration [1]. Hence, for example, for cell-averaged u velocity

$$\frac{1}{2a_i} \int_{-a_i}^{a_i} \bar{u}^{yzt}(x) dx = \frac{1}{2b_j} \int_{-b_j}^{b_j} \bar{u}^{xzt}(y) dy = \frac{1}{2c_k} \int_{-c_k}^{c_k} \bar{u}^{xyt}(z) dz = \frac{1}{2\tau_n} \int_{-\tau_n}^{\tau_n} \bar{u}^{xyz}(t) dt . \quad (30)$$

Eliminating the pseudo-source terms using these constraint equations leads to a final set of fifteen equations and fifteen unknowns per cell.

2.5. New Features of MNIM

As in the two-dimensional modified nodal integral method, three characteristics of the numerical scheme differentiate the MNIM from the conventional nodal integral method. First, the local solution of transverse averaged velocities has a component that varies exponentially in space. These exponential terms can capture steep spatial variation of velocities within each cell, thus, allowing the use of coarse meshes. Second, because of the appearance of the local Reynolds number in the exponential terms, the scheme developed here has inherent upwinding. Moreover, local Reynolds number based only on previous time step velocities appear as argument of the exponential terms. Hence, these terms can be evaluated at the beginning of each time step outside the iteration loop, which significantly reduces the computation time. Third, local transverse-integrated velocities in all directions have the same *constant + linear + exponential* functional form. Hence, unlike the NIM, the MNIM leads to a set of discrete equations that are symmetric in x , y and z directions.

2.6. Code Implementation of MNIM

This set of equations has been implemented in a Fortran code, and tested on several three-dimensional fluid flow problems. Steady-state problems are solved by marching in time. Several iterative approaches have been tested to solve the final set of algebraic equations at each time step. Results presented are based on a SIMPLE-like algorithm. Gauss-Seidel iterations are used for each field variable. That is, for fixed pressure field, velocities are evaluated row by row over the whole domain. Next, keeping velocities fixed, discrete pressure values are evaluated row by row over the entire domain. For given velocity field, around fifteen pressure-sweeps yield near optimum convergence. As is the case with many other iterative approaches, for given pressure field only a single sweep to update the velocity was found to be sufficient.

3. NUMERICAL RESULTS

We here report the results for the three-dimensional, lid driven cavity problems [10-13], in which the lid at the top ($z = 1$ for cubic and $z = 2$ for prism) moves with a constant velocity in the x direction (see Fig.1). Figures 2 and 3 illustrate the u and w velocities along the center line parallel to the z -axis and x -axis respectively for Reynolds number of 100. Figures 4 and 5 are corresponding velocity profiles for Reynolds number of 1000. These results are obtained using a $20 \times 20 \times 20$ non-uniform mesh and are compared with those from Ref. 11 and 12 in Figures 2-5. It is clear from these results that even for coarse meshes, the MNIM for the time-dependent N-S equations leads to fairly accurate results. For the $Re = 1000$ case, Babu et al. [12] used an $81 \times 81 \times 81$ mesh, while a $20 \times 20 \times 20$ mesh is used in MNIM. The MNIM code takes about 60 minutes for $Re = 100$ and 126 minutes for $Re = 1000$ on a 1.5 GHz PC running LINUX operating system. The CPU time is low despite the fact that very simple Gauss-Seidel sweeps are used repeatedly at each time step till convergence. For larger problems, significant savings in CPU time can be achieved by incorporating more efficient solvers.

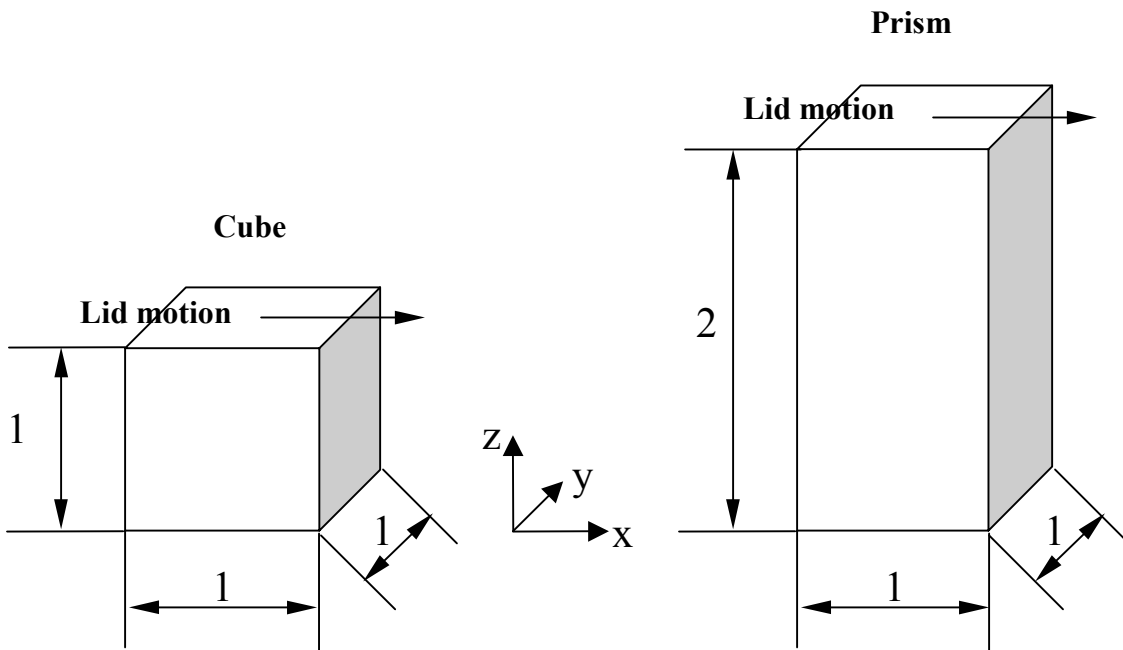


Figure 1. Configuration of the lid driven cavity problem

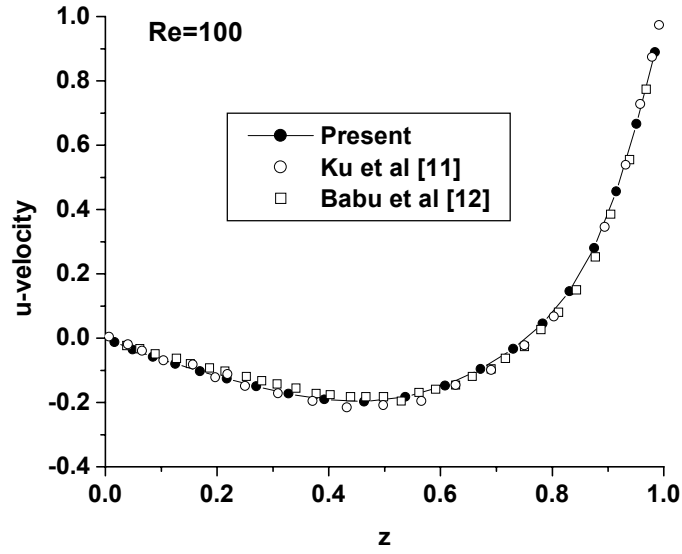


Figure 2. U-velocity along the vertical centerline for the 3D lid driven cavity problem.

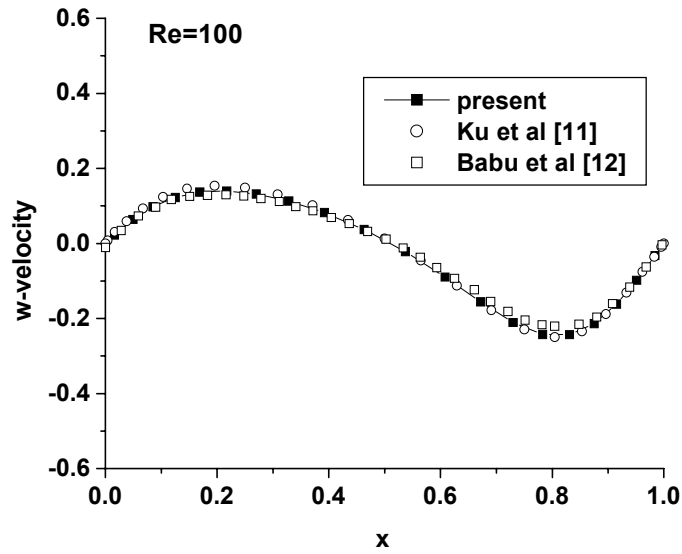


Figure 3. W-velocity along the horizontal centerline for the 3D lid driven cavity problem.

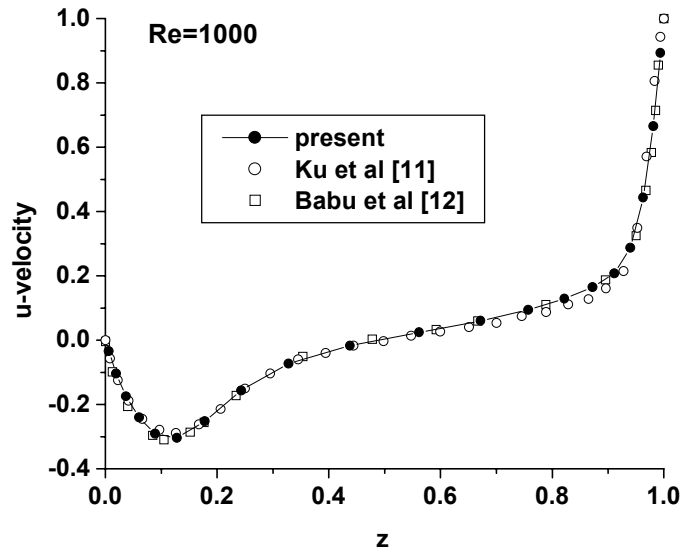


Figure 4. U-velocity along the vertical centerline for the 3D lid driven cavity problem.

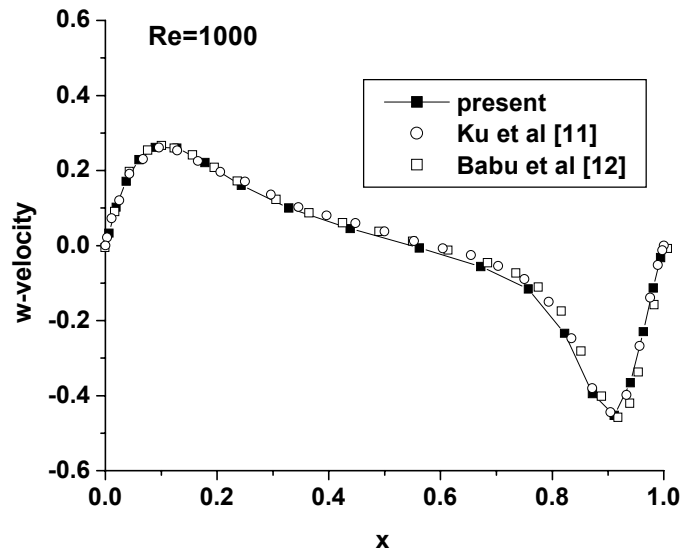


Figure 5. W-velocity along the horizontal centerline for the 3D lid driven cavity problem.

In the prism case, a $20 \times 20 \times 40$ nonuniform mesh with a geometric factor of 1.1 was used for MNIM. The MNIM results agree very well with the reference solution (see Fig. 6), which was obtained using $35 \times 35 \times 70$ mesh [13]. A time step of 0.03 is used and steady state is reached after 300 time steps. The reference solution [13] on the other hand was obtained using time step of 0.00025 and 60000 time steps.

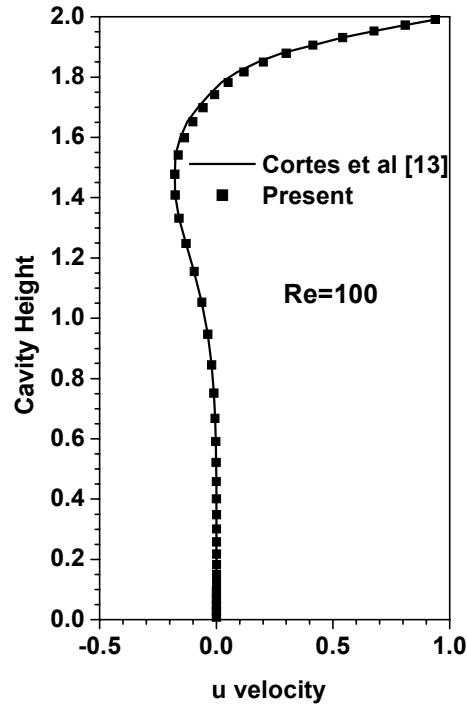


Figure 6. Comparison of centerline velocity profiles for a prismatic cavity with an aspect ratio of 2 at Reynolds number of 100

4. SUMMARY

A modified nodal integral method for three-dimensional time-dependent Navier-Stokes equations is developed. It is an extension of the two-dimensional scheme reported recently. Results obtained using the modified scheme are compared with those reported in literature for three-dimensional lid driven cavity problems in cube and prism shaped cavities. Good agreement is found between results obtained here and reference solution. Moreover, grid size used in the MNIM is much coarser than those used earlier to solve the same problems.

ACKNOWLEDGEMENT

Research funded in part by the U.S. Department of Energy through the University of California under subcontract number B341494. First author (FW) would also like to acknowledge support under the Computational Science and Engineering Fellowship program at University of Illinois at Urbana Champaign.

REFERENCES

1. Y.Y. Azmy and J.J. Dorning, "A Nodal Integral Approach to the Numerical Solution of Partial Differential Equations," in *Advances in Reactor Computations*, volume II, pages 893-909. American Nuclear Society, LaGrange Park, IL (1983).
2. G.L. Wilson, R.A. Rydin, and Y.Y. Azmy, "Time-Dependent Nodal Integral Method for the Investigation of Bifurcation and Nonlinear Phenomena in Fluid Flow and Natural Convection," *Nucl. Sci. Eng.* **100**, 414-425 (1988).
3. P.D. Esser, R.J. Witt, "An Upwind Nodal Integral Method for Incompressible Fluid Flow," *Nuclear Science and Engineering*, **114**, 20-35(1993).
4. E.P.E. Michael and J.J. Dorning, "A Primitive-Variable Nodal Method for Steady-State Fluid Flow," *Trans. Am. Nuc. Soc.*, **83**, p. 420-422 (2000).
5. Fei Wang and Rizwan-uddin, "A Nodal Scheme for the Time-Dependent, Incompressible Navier-Stokes Equations," *Trans. Amer. Nucl. Soc.*, **83**, 422-424 (2000). Also, to appear in *Journal of Computational Physics*.
6. R.D. Lawrence, "Progress in Nodal Methods for the Solutions of the Neutron Diffusion and Transport Equations," *Progress in Nuclear Energy*, **17** (3), 271-301 (1986).
7. A.J. Toreja and Rizwan-uddin, "Hybrid Numerical Methods for the Convection-Diffusion Equation in Arbitrary Geometries," in the Proc. *M&C-99 International Conference on Mathematics and Computation, Reactor Physics and Environmental Analysis in Nuclear Applications*, [Madrid, Spain, September, 27-30, 1999], Ed. J.M. Aragonés, pp. 1705-1714, Senda Editorial, Madrid (1999).
8. J.C. Tannehill, D.A. Anderson and R.H. Pletcher, *Computational Fluid Mechanics and Heat Transfer* (2nd Ed), Taylor and Francis (1997).
9. K.N. Ghia, W.L. Hankey Jr. and J.K. Hodge, "Study of Incompressible Navier-Stokes Equations in Primitive Variables Using Implicit Numerical Technique," AIAA Paper 77-648 (1977).
10. A. Baloch, P.W. Grant and M.F. Webster, "Homogeneous and Heterogeneous Distributed Cluster Processing for two and Three-Dimensional Viscoelastic Flows," *International Journal for Numerical Methods in Fluids*, **40**, 1347-1363 (2002)
11. Hwar C. Ku, Richard S. Hirsh and Thomas D. Taylor, "A Pseudospectral Method for Solution of the Three-Dimensional Incompressible Navier-Stokes Equations," *Journal of Computational Physics*, **70**, 439-462 (1987)
12. V. Babu and Seppo A. Korpela, "Numerical Solution of the Incompressible, Three-Dimensional Navier-Stokes Equations," *Computers Fluids*, **23**, 675-691 (1994)
13. A. B. Cortes and J. D. Miller, "Numerical Experiments with the Lid Driven Cavity Flow Problem," *Computers Fluids*, **23**, 1005-1027 (1994)